Amino Acids (2015) 47:885–898
DOI 10.1007/s00726-015-1916-2

ORIGINAL ARTICLE

Effect of charged amino acid side chain length on lateral cross-strand interactions between carboxylate- and guanidinium-containing residues in a β-hairpin

Hsiou-Ting Kuo · Shing-Lung Liu · Wen-Chieh Chiu · Chun-Jen Fang · Hsien-Chen Chang · Wei-Ren Wang · Po-An Yang · Jhe-Hao Li · Shing-Jong Huang · Shou-Ling Huang · Richard P. Cheng

Received: 30 August 2014 / Accepted: 6 January 2015 / Published online: 3 February 2015

Abstract β-Sheet is one of the major protein secondary structures. Oppositely charged residues are frequently observed across neighboring strands in antiparallel sheets, suggesting the importance of cross-strand ion pairing interactions. The charged amino acids Asp, Glu, Arg, and Lys have different numbers of hydrophobic methylenes linking the charged functionality to the backbone. To investigate the effect of side chain length of guanidinium- and carboxylate-containing residues on lateral cross-strand ion pairing interactions at non-hydrogen-bonded positions, β-hairpin peptides containing Zbb-Agx (Zbb = Asp, Glu, Aad in increasing length; Agx = Agh, Arg, Agb, Agp in decreasing length) sequence patterns were studied by NMR methods. The fraction folded population and folding energy were derived from the chemical shift deviation data. Peptides with high fraction folded populations involved charged residue side chain lengths that supported high strand propensity. Double mutant cycle analysis was used to determine the interaction energy for the potential lateral ion pairs. Minimal interaction was observed between residues with short side chains, most likely due to the diffused positive charge on the guanidinium group, which weakened cross-strand electrostatic interactions with the carboxylate side chain. Only the Aad-Arg/Agh interactions with long side chains clearly exhibited stabilizing energetics, possibly relying on hydrophobics. A survey of a non-redundant protein structure database revealed that the statistical sheet pair propensity followed the trend Asp-Arg < Glu-Arg, implying the need for matching long side chains. This suggested the need for long side chains on both guanidinium-bearing and carboxylate-bearing residues to stabilize the β-hairpin motif.

Keywords Carboxylate · Guanidinium · Side chain length · β-Hairpin · Ion pairing interaction

Abbreviations

Aad	(*S*)-Aminoadipate
Agb	(*S*)-2-Amino-4-guanidinobutyric acid
Agh	(*S*)-2-Amino-6-guanidinohexanoic acid
Agp	(*S*)-2-Amino-3-guanidinopropionic acid
Ala	Alanine
Arg	Arginine
Asp	Aspartate
DQF-COSY	Double-quantum filtered-correlated spectroscopy
Fmoc	N^{α}-Fluorenylmethyloxycarbonyl
Glu	Glutamate
Lys	Lysine
MALDI-TOF	Matrix-assisted laser desorption ionization time-of-flight
NMR	Nuclear magnetic resonance spectroscopy
NOESY	Nuclear overhauser effect spectroscopy
Orn	Ornithine
ROESY	Rotating-frame nuclear Overhauser effect spectroscopy
TOCSY	Total correlation spectroscopy

Handling Editor: P. Kursula.

Electronic supplementary material The online version of this article (doi:10.1007/s00726-015-1916-2) contains supplementary material, which is available to authorized users.

H.-T. Kuo · S.-L. Liu · W.-C. Chiu · C.-J. Fang · H.-C. Chang · W.-R. Wang · P.-A. Yang · J.-H. Li · R. P. Cheng (✉)
Department of Chemistry, National Taiwan University, Taipei 10617, Taiwan
e-mail: rpcheng@ntu.edu.tw

S.-J. Huang · S.-L. Huang
Instrument Center at National Taiwan University, National Taiwan University, Taipei 10617, Taiwan

Introduction

Protein misfolding can lead to various human neurological disorders including Alzheimer's disease (Hardy and Allsop 1991; Bartzokis et al. 2007), Huntington's disease (Scherzinger et al. 1997; Truant et al. 2008), Parkinson's disease (Irvine et al. 2008; Mastaglia et al. 2003), type II diabetes (Höppener et al. 2000; Haataja et al. 2008), and Creutzfeldt-Jakob prion disease (Kitamoto et al. 1986; Namba et al. 1991). The protein misfolded conformation in these diseases involves the β-sheet structure, which is formed during amyloid fibril formation. The β-sheet structure is one of the major secondary structures (Baldwin and Rose 1999a, b), with 23 % of the protein residues adopting a β-sheet conformation (Chou and Fasman 1974; Munoz and Serrano 1994; Kuo et al. 2013b). Statistical analysis of protein structures (Wouters and Curmi 1995; Cootes et al. 1998; Hutchinson et al. 1998) suggests that cross-strand side chain–side chain interactions between two β-strands are important for stabilizing sheet structures (Wouters and Curmi 1995; Cootes et al. 1998; Hutchinson et al. 1998). Accordingly, various cross-strand interactions have been studied, including cation–π (Tatko and Waters 2003; Hughes et al. 2007; Syud et al. 2001), hydrophobics (Searle et al. 1999; Tatko and Waters 2004), electrostatics (de Alba et al. 1995; Searle et al. 1999; Kiehna and Waters 2003; Ramirez-Alvarado et al. 2001), van der Waals (Paliwal et al. 1994; Kim et al. 1998), aromatic π–π (Tatko and Waters 2002; Kiehna and Waters 2003), and carbohydrate–π (Laughrey et al. 2008).

The energetics of cross-strand ion pairs have been measured in sheet-containing host systems including the protein G B1 domain (Smith and Regan 1995; Merkel et al. 1999), the zinc finger domain (Blasie and Berg 1997), and also in autonomously folded β-hairpins (Searle et al. 1999; Russell and Cochran 2000; Syud et al. 2001; Ramirez-Alvarado et al. 2001; Kiehna and Waters 2003; Ciani et al. 2003). For the protein G B1 domain host, both lateral cross-strand Glu-Lys and Glu-Arg interactions provided around 1 kcal/mol stability based on the thermal denaturation studies (Smith and Regan 1995). For the zinc finger domain host, cross-strand ion pairing interactions involving Asp were more stabilizing than those involving Glu (Blasie and Berg 1997). Furthermore, cross-strand Lys-Asp and Arg-Asp interactions stabilized the system by 0.48 and 0.26 kcal/mol (Blasie and Berg 1997), respectively. In short hairpin peptides, lateral cross-strand Glu-Lys ion pairing interactions increased the hairpin stability by 0.1–0.3 kcal/mol based on NMR methods (Ramirez-Alvarado et al. 2001; Kiehna and Waters 2003; Ciani et al. 2003; Kuo et al. 2013a). The effect of charged amino acid side chain length on lateral cross-strand glutamate-lysine ion pairing interaction in a β-hairpin has also been explored in detail (Kuo et al. 2013a). Combinations with shorter side chains for both charged residues such as Asp/Glu-Dap ion pairs and longer side chains for both charged residues such as Aad-Orn/Lys ion pairs stabilized the β-hairpin structure (Kuo et al. 2013a). The shorter Asp/Glu-Dap interactions exhibited stabilizing energetics most likely due to electrostatics, whereas the longer Aad-Orn/Lys interactions were stabilizing most likely due to hydrophobics (Kuo et al. 2013a). As such, side chain length matching for the Lys and Glu analogs on separate strands appeared to be important for providing stabilizing energetics in β-hairpin structures.

The charged amino acids Asp, Glu, Arg, and Lys have different number of hydrophobic methylenes linking the hydrophilic charged functionality to the backbone. The negatively charged residues Asp and Glu both bear the same carboxylate functionality, and only differ in the number of methylenes. Arginine and lysine are positively charged residues with different number of methylenes. Furthermore, Arg is different from Lys in bearing a guanidinium group to carry the positive charge instead of an ammonium group. This creates a more diffuse positive charge, higher hydrogen bonding capacity, and different geometry for Arg compared to the Lys ammonium group. As such, Arg cannot be replaced with Lys in many cases (such as for cell penetration) due to the uniqueness of the guanidinium group on Arg (Wender et al. 2000, 2008; Mitchell et al. 2000; Janin et al. 1988; Argos 1988; Jones and Thornton 1995; Tsai et al. 1997; Bogan and Thorn 1998; Hu et al. 2000; Arora and Khanna 1996; de Bernardez 1998; Umetsu et al. 2003; Arakawa and Tsumoto 2003; Tsumoto et al. 2004; Singh and Panda 2005; Ito et al. 2008). The difference between Arg and Lys is also reflected in the thermodynamic secondary structure propensities (Padmanabhan et al. 1996; Cheng et al. 2012b; Kuo et al. 2013b). The helix propensity increased as the side chain lengths of Lys analogs increased (Chakrabartty et al. 1994; Doig and Baldwin 1995; Sueki et al. 1984; Padmanabhan et al. 1996). In contrast, either shortening or lengthening the Arg side chain length decreased the helix propensity (Cheng et al. 2012b). As for strand propensity measured in a β-hairpin model system (Kuo et al. 2013b), the stability of the β-hairpin motif increased upon increasing the Lys analog side chain length (Hughes et al. 2007; Kuo et al. 2013b), whereas the stability trend for the Arg analogs varied depending on the position (Kuo et al. 2013b). Lengthening the Arg side chain by one methylene favored β-strand formation (Kuo et al. 2013b), whereas shortening the side chain of Arg by one methylene disfavored β-strand formation (Kuo et al. 2013b). Interestingly, shortening the Arg side chain by two methylenes resulted in higher or similar sheet propensity compared to Arg depending on the position in the β-hairpin (Kuo et al. 2013b). Overall, Arg and Lys are significantly different, and should have different

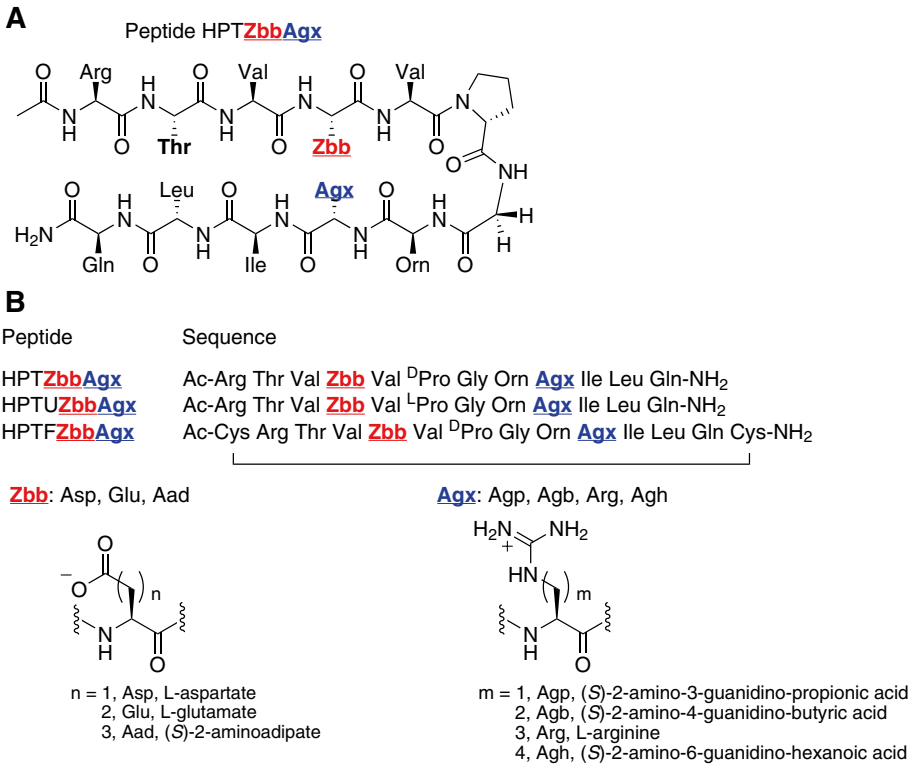

Fig. 1 Design of peptides to study the effect of charged amino acid side chain length on lateral ion pairing interactions. **a** The chemical structure of the experimental HPTZbbAgx peptides. **b** The sequences of the experimental HPTZbbAgx peptides, the unfolded reference HPTUZbbAgx peptides, and the folded reference HPTFZbbAgx peptides

effects on protein structure stability. Therefore, herein we present a systematic study on β-hairpin peptides containing potential lateral cross-strand ion pairs between positively charged Arg analogs and negatively charged Glu analogs with varying side chain lengths using NMR methods. The interaction energy was determined by double mutant cycle analysis, and a non-redundant protein structure database was surveyed for sequence patterns with oppositely charged residues (Arg and Asp/Glu) directly across one another in antiparallel β-sheets.

Results

Peptide design and synthesis

The sequences for the experimental HPTZbbAgx peptides were the same as previously studied hairpin peptides (Fig. 1) (Kuo et al. 2013a, b), which were designed based on Gellman's peptide YKL (H-Arg-Tyr-Val-Glu-Val-DPro-Gly-Orn-Lys-Ile-Leu-Gln-NH_2) (Stanger and Gellman 1998; Syud et al. 1999, 2001). Tyr2 was replaced with Thr (Kuo et al. 2013a, b), because the two amino acids exhibited similar thermodynamic sheet propensities (Kim and Berg 1993; Minor and Kim 1994; Smith et al. 1994). The N- and C-termini were capped by an acetyl group and carboxyamide (Kuo et al. 2013a), respectively, to minimize unintended electrostatic interactions involving the charged termini (Fig. 1) (Searle et al. 1999). The guest sites for the negatively charged and positively charged residues were the non-hydrogen bonding positions 4 and 9, respectively. The negatively charged amino acids (Zbb) with varying side chain lengths were incorporated at position 4 (Fig. 1). The negatively charged residue Zbb was systematically lengthened from Asp (one methylene) to Glu (two methylenes), and then to (*S*)-2-aminoadipate (Aad, three methylenes) (Fig. 1b). The positively charged amino acids (Agx) with varying side chain lengths were incorporated at position 9 (Fig. 1). The guanidinium-bearing positively charged residue Agx was systematically shortened from (*S*)-2-amino-6-guanidinohexanoic acid (Agh, 4 methylenes) to Arg (3 methylenes), to (*S*)-2-amino-4-guanidinobutyric acid (Agb, 2 methylenes), and to (*S*)-2-amino-3-guanidinopropionic acid (Agp, 1 methylene) (Fig. 1b). The hairpin HPTZbbAgx peptides were named according to the one-letter code of Thr at position 2 and the three-letter code of the potentially interacting negatively and positively charged residues. Fully unfolded and folded reference peptides were necessary to determine the fraction folded population for the experimental HPTZbbAgx peptides (Syud et al. 2001; Tatko and Waters 2002, 2003; Syud et al. 1999; Kuo et al. 2013a, b). The unfolded reference peptides HPT**U**ZbbAgx were designed by changing the turn sequence from D-Pro to L-Pro to disrupt the β-hairpin conformation (Fig. 1b)

(Rose et al. 1985; Syud et al. 1999; Kuo et al. 2013a, b). The folded reference peptides HPTFZbbAgx were designed by introducing cysteines at both the N- and C-terminus for cyclization via disulfide bond formation (Fig. 1b) (Syud et al. 2001; Tatko and Waters 2002, 2003; Syud et al. 1999; Kuo et al. 2013a, b).

The peptides were synthesized by solid phase peptide synthesis using Fmoc-based chemistry (Fields and Noble 1990; Atherton et al. 1978). Peptides containing (*S*)-2-amino-6-guanidinohexanoic acid (Agh) were synthesized by standard coupling protocols using Fmoc-Agh(Boc)$_2$-OH (Cheng et al. 2012b; Wu et al. 2013). Peptides containing (*S*)-2-amino-4-guanidinobutanoic acid (Agb) were synthesized by solid phase guanidinylation (Cheng et al. 2012b; Wu et al. 2013). However, peptides containing (*S*)-2-amino-3-guanidinopropanoic acid (Agp) could not be synthesized by solid phase guanidinylation using the precursor Fmoc-Dap(Mtt)-OH for this β-hairpin system (Cheng et al. 2012b; Wu et al. 2013). After synthesizing the corresponding Dap(Mtt)-containing peptides, the Mtt protecting group was selectively removed using 1 % trifluoroacetic acid/methylene chloride followed by solid phase guanidinylation using *N*,*N'*-di-Boc-*N"*-triflylguanidine in the presence of diisopropylethylamine under microwave conditions (Cheng et al. 2012b; Wu et al. 2013). However, some of the Boc-protecting groups on Orn in this β-hairpin sequence were also removed upon exposure to even 1 % trifluoroacetic acid in methylene chloride. As such, the guanidinium group was introduced onto the side chain of both Dap and Orn. The synthetic route involving the Fmoc-Dap(ivDde)-OH for the Agp-containing peptide was not explored, because side chain to main chain migration may occur with Dap(ivDde)-containing peptides during solid phase peptide synthesis (Augustyns et al. 1998). Accordingly, it was more suitable to use Fmoc-Agp(Boc)$_2$-OH to synthesize the Agp-containing peptides by standard Fmoc-based solid phase peptide synthesis. The appropriately protected Agp-derivative was synthesized following known published procedures using a *N*-triflylguanidine derivative (Feichtinger et al. 1998a, b; Cheng et al. 2012b). The short side chain length of Fmoc-Agp(Boc)$_2$-OH positions the Boc-protecting groups in close proximity to the backbone, resulting in significant steric hindrance. Therefore, for incorporating Agp residues, Fmoc-Agp(Boc)$_2$-OH was coupled multiple times under microwave conditions. Upon cleavage with concomitant side chain deprotection, the peptides were confirmed by MALDI-TOF mass spectrometry. The folded reference HPTFZbbAgx peptides were cyclized by disulfide bond formation via charcoal mediated air oxidation (Volkmer-Engert et al. 1998). All peptides were purified by reverse-phase high-performance liquid chromatography to greater than 95 % purity. Since the NMR spectra (chemical shift and line width) of analogous hairpin peptides did not change with concentration (20 μM–10 mM) (Syud et al. 2001; Ramirez-Alvarado et al. 1996; Russell et al. 2003; Kuo et al. 2013a, b), the peptides in this study (2.5–10.4 mM) should not aggregate in solution. Accordingly, the experimental data should reflect the intra-molecular interactions with minimal interference from inter-molecular interactions.

β-Hairpin structure characterization by NMR

The peptides were analyzed by two-dimensional NMR spectroscopy including TOCSY (Bax and Davis 1985), DQF-COSY (Aue et al. 1976), NOESY (Jeener et al. 1979), and ROESY (Bothner-By et al. 1984) at 298 K. Sequence specific assignments of the chemical shifts were performed based on the TOCSY and ROESY spectra (Tables S1–S36) (Wüthrich 1986). The chemical shift dispersion trends were consistent with the intended designs of the peptides (Tables S1–S36) (Kuo et al. 2013a; Yao et al. 1997). The higher the fraction folded population, the higher the chemical shift dispersion (Kuo et al. 2013a, b; Yao et al. 1997). The hairpin structure and stability of the HPTZbbAgx and HPTFZbbAgx peptides was confirmed by Hα chemical shift deviations (ΔδHα) (Dalgarno et al. 1983; Wishart et al. 1991), $^3J_{NH\alpha}$ spin–spin coupling constants, and cross-strand NOEs (Kuo et al. 2013a, b). The ΔδHα values of the experimental HPTZbbAgx peptides and folded reference HPTFZbbAgx peptides represented the degree of β-sheet structure at each position (Figs. 2, S1, S2) (Syud et al. 2001). Residues Thr2 through Val5 and Orn8 through Leu11 exhibited significantly positive ΔδHα values (Figs. 2, S1, S2), suggesting that the HPTZbbAgx and HPTFZbbAgx peptides displayed reasonable β-hairpin populations. The ΔδHα values of the terminal residues Arg1 and Gln12 were near zero due to end fraying effects (Ciani et al. 2003). The ΔδHα values for DPro6 and Gly7 were mostly close to zero, suggesting turn formation (Ramirez-Alvarado et al. 1996).

The $^3J_{NH\alpha}$ spin–spin coupling constant for the residues in the peptides was derived from the DQF-COSY spectra (Kim and Prestegard 1989). In the folded reference HPTFZbbAgx peptides, the $^3J_{NH\alpha}$ values for all residues except cysteine and glycine were higher than 7 Hz (Tables S37–S39), consistent with a β-sheet conformation (Wüthrich 1986). The experimental HPTZbbAgx peptides exhibited similar results but slightly lower $^3J_{NH\alpha}$ values for some residues (Tables S40–S42). Although this suggested that the experimental peptides formed a β-hairpin conformation, the structure may not be as well defined as the folded reference peptides. Regarding the unfolded reference HPTUZbbAgx peptides, some residues exhibited $^3J_{NH\alpha}$ values near to or less than 7 Hz, suggesting that the peptides may not form a well-defined β-hairpin and are thus most likely unfolded (Tables S43–S45).

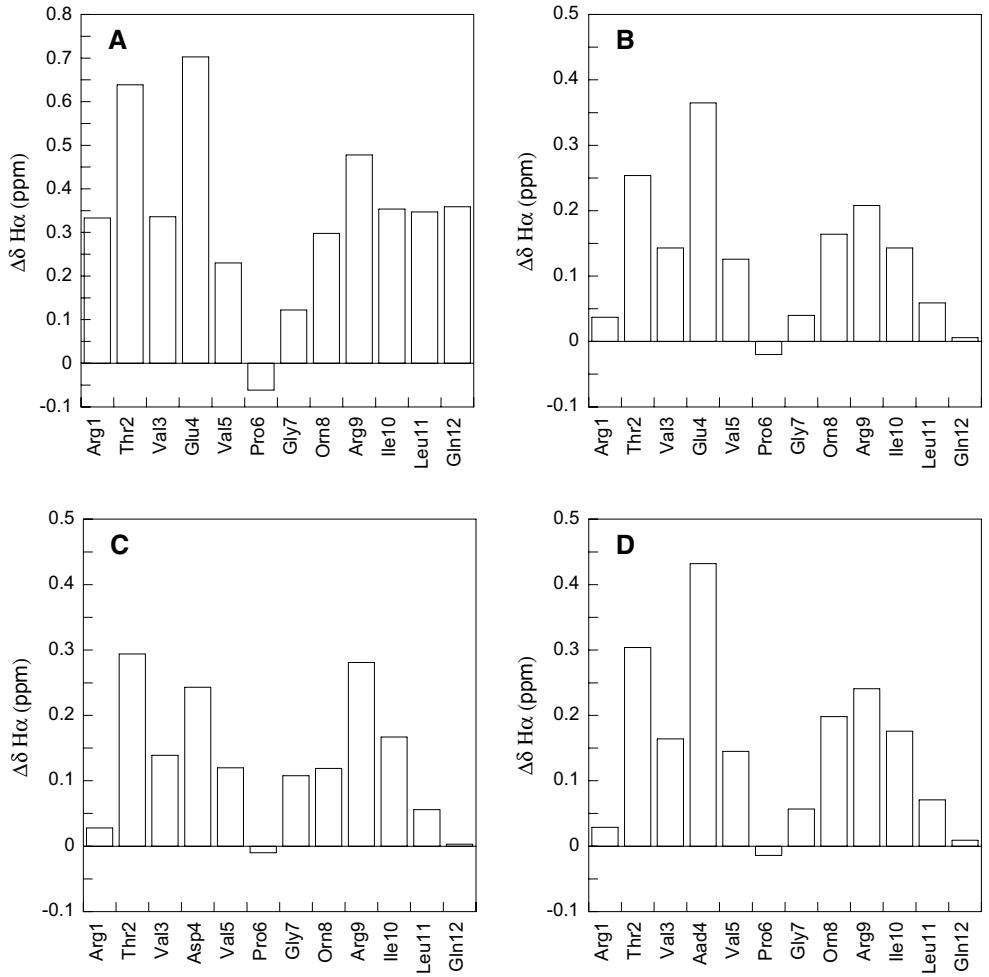

Fig. 2 The chemical shift deviation (ΔδHα) for the residues in peptides HPTFGluArg (**a**), HPTGluArg (**b**), HPTAspArg (**c**), and HPTAadArg (**d**)

Cross-strand NOE connectivities observed in the ROESY spectra further supported β-hairpin formation. The NOE cross peaks included sequential, intra-residues, medium-range, and long-range NOEs with a number of cross-strand Hα ↔ Hα, Hα ↔ NH, NH ↔ NH correlations to confirm the peptide conformation (Figs. S3–S26). The β-strand structures were confirmed by diagnostic NOEs; the strong sequential $H\alpha_i \leftrightarrow NH_{i+1}$ NOEs suggested an extended and stretched conformation. The network of side chain–side chain NOEs between residues on the two adjacent β-strands further confirmed the β-hairpin formation for the experimental HPTZbbAgx peptides and folded reference HPTFZbbAgx peptides (Figs. S3–S14). The side chain of Thr2 exhibited lateral hydrophobic contacts to Leu11, especially in the folded reference HPTFZbbAgx peptides (Figs. S3–S14). Furthermore, the long-range diagonal cross-strand NOEs connectivities between Thr2 and Agx9 were clearly observed in the experimental HPTZbbAgx peptides (Figs. S3–S14), consistent with the typical right-handed twist of β-hairpin structures (Syud et al. 2001; Ramirez-Alvarado et al. 1999; Syud et al. 1999; Ramirez-Alvarado et al. 1996). The side chain of the two oppositely charged residues, Zbb4 with carboxylate groups and Agx9 with guanidinium groups, also showed cross-strand NOE connectivities to one another in some cases (Figs. S3–S14). The number of cross peaks in the ROESY spectra followed the general trend HPTFZbbAgx > HPTZbbAgx > HPTUZbbAgx (Figs. S3–S26), consistent with the intended fraction folded population for the peptides (Kuo et al. 2013a, b).

Fraction folded population and ΔG_{fold}

The fraction folded population and folding free energy (ΔG_{fold}) for each residue on the experimental HPTZbbAgx peptides were derived from the Hα chemical shift data (Figs. S27, S28). The fraction folded population of the residues at the N- and C-termini was very low, most likely

Table 1 The fraction folded population (%) for the HPTZbbAgx peptides

Zbb			
Agx	Asp	Glu	Aad
Agp	52 ± 1	47 ± 1	37 ± 2
Agb	53 ± 1	31 ± 2	28 ± 3
Arg	49 ± 3	42 ± 2	49 ± 2
Agh	56 ± 3	47 ± 1	52 ± 1

The general sequence for the HPTZbbAgx peptides is Ac-Arg-Thr-Val-Zbb-Val-DPro-Gly-Orn-Agx-Ile-Leu-Gln-NH_2. Average value for residues 2, 3, 9, and 10

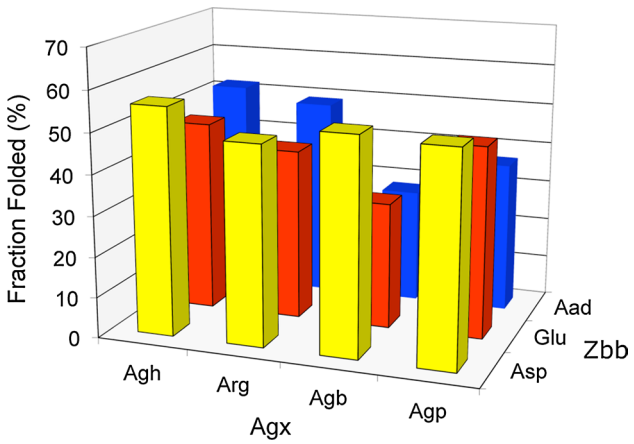

Fig. 3 The fraction folded population for HPTZbbAgx peptides

due to end fraying effects (Fig. S27). On the contrary, the residues directly adjacent to the turn exhibited high fraction folded population due to turn-promoted sheet formation (Fig. S27). Accordingly, residues Thr2, Val3, Agx9, and Ile10 were chosen to represent the fraction folded population for a given peptide (Tables 1; Fig. 3) (Kuo et al. 2013a). These residues were selected to provide equal representation for the hydrogen-bonded (3 and 10) and non-hydrogen-bonded positions (2 and 9) on the two strands, and account for the apparent uneven folding of the two strands due to the inherent right-handed twist.

The range of the fraction folded population for the HPTZbbAgx peptides was between 28 and 56 % with standard deviations within 3 % (Table 1). Peptides containing Agb (two methylenes) exhibited the least fraction folded population (accounting for the standard deviations) for a given negatively charged residue (Table 1). This mirrors the strand propensity for the positively charged residue Agx at position 9 (with Ala at position 4) (Kuo et al. 2013b). For the HPTGluAgx peptides, the fraction folded population increased with increasing side chain length of the positively charged Arg analog, except for the shortest residue Agp (Table 1; Fig. 3). A similar trend was observed for the HPTAadAgx peptides; the stability seemed to roughly increase with increasing the Agx side chain length from two to four methylenes (Agb, Arg, and Agh) (Table 1; Fig. 3). Interestingly, the peptide HPTGluAgp with the shortest positively charged residue showed an exceptionally high fraction folded population, similar to that for the peptide HPTGluAgh with the longest positively charged residue. Furthermore, the fraction folded population for the HPTAadAgx peptides followed the trend HPTAadAgb < HPTAadAgp < HPTAadArg < HPTAadAgh. The fraction folded population of peptide HPTAadAgp peptide with the shortest positively charged residue was less than that for peptide HPTAadArg. However, the strand propensity of the shortest residue Agp (one methylene) (and Ala at position 4) was similar to that of Arg (three methylenes) at position 9 (Kuo et al. 2013b). Apparently, the fraction folded population of the HPTGluAgx and HPTAadAgx peptides did not strictly follow the strand propensity trends. Among the HPTAspAgx peptides, the peptide with the longest positively charged residue Agh (HPTAspAgh) exhibited the highest fraction folded population, consistent with the highest strand propensity for Agh at position 9 (Kuo et al. 2013b). Furthermore, peptide HPTAspAgh exhibited the highest fraction folded population among all the HPTZbbAgx peptides. In contrast, the peptide with the natural residue Arg (HPTAspArg) interestingly exhibited the least fraction folded population. Furthermore, by shortening the side chain of Arg to Agb and Agp, the fraction folded population did not alter significantly. Accordingly, the trend of the fraction folded population for HPTAspAgx peptides was very different from the trend for the strand propensity of the Arg analogs at position 9. The fraction folded population for the Asp-containing peptides was higher than or equal to that for the corresponding Glu- and Aad-containing peptides. This was consistent with the strand propensity for the negatively charged residues at position 4 (Kuo et al. 2013b).

Lateral cross-strand Zbb-Agx interactions

The interaction free energy (ΔG_{int}) for each lateral Zbb-Agx interaction between oppositely charged residues was derived from the corresponding double mutant cycle (Table 2) (Horovitz 1996; Cockroft and Hunter 2007). Double mutant cycles were employed to exclude the effect of altering the side chain length on β-strand propensity of the individual charged residues and the potential diagonal Thr2-Agx9 interaction. The free energy of interaction (ΔG_{int}) for each charged pair was derived from the difference between the free energy changes observed for the singly substituted control peptides [(HPTZbbAla (Kuo et al. 2013b) and HPTAlaAgx (Kuo et al. 2013b)] and the free

Table 2 The Zbb-Agx interaction free energy (ΔG_{int}, kcal/mol) in HPTZbbAgx peptides

Agx	Zbb		
	Asp	Glu	Aad
Agp	−0.03 ± 0.20	−0.13 ± 0.21	−0.03 ± 0.21
Agb	−0.26 ± 0.26	0.04 ± 0.27	0.02 ± 0.28
Arg	0.11 ± 0.18	0.06 ± 0.18	−0.25 ± 0.19
Agh	0.04 ± 0.19	0.03 ± 0.18	−0.22 ± 0.19

energy changes observed for experimental HPTZbbAgx peptides ($\Delta\Delta G_{HPTZbbAgx}$) compared to the reference control peptide HPTAlaAla (Kuo et al. 2013a). The interaction energy between two charged residues is a relative but not absolute value between one state and another state (Horovitz 1996). Accordingly, the almost non-existent ion pairing interactions ($\Delta G_{int} = 0$ or >0, Table 2) for cross-strand lateral Zbb-Agx with various side chain length only indicates no variation in coupling energy between the charged residues Zbb and Agx from one state to another, but does not mean that the two residues are not coupled to each other (Horovitz 1996). Interestingly, only two cross-strand lateral ion pairing interactions were clearly stabilizing: Aad-Agh, and Aad-Arg. The longest negatively charged residue Aad paired with the longer positively charged residues Agh and Arg provided the highest stabilizing interaction energy for the Zbb-Agx lateral cross-strand interactions. Surprisingly, the short side chain lengths for oppositely charged residues with lateral cross-strand arrangements did not appear to stabilize the β-hairpin structure. This suggests that side chain length matching of the longer oppositely charged residues is important for forming stabilizing lateral cross-strand interactions between carboxylate- and guanidinium-containing residues.

Discussion

The Arg guanidinium group exhibits a more diffuse positive charge, higher hydrogen bonding capacity, and different geometry compared to the Lys ammonium group (Fig. 1). Despite these differences between Lys and Arg, short helical peptides with either Zbb-Lys or Zbb-Arg (i, $i + 3$), (i, $i + 4$), and (i, $i + 5$) sequence patterns exhibited significant helical content at pH 7, regardless of the negatively charged residue side chain length (Cheng et al. 2007, 2012a; Kuo et al. 2014). Furthermore, the strand propensity in a β-hairpin mostly increased with increasing side chain length for the positively charged Lys and Arg analogs except for Agp (Kuo et al. 2013b). The strand propensity of Agp was unexpectedly higher than the longer Agb despite the shorter side chain length (Kuo et al. 2013b). Accordingly, the Arg analogs should behave somewhat differently compared to the Lys analogs in ion pairing interactions involving sheet structures. As such, the effect of side chain length on lateral ion pairing interactions between carboxylate and guanidinium amino acids at non-hydrogen-bonded positions on different strands of a β-hairpin was investigated in this study.

The fraction folded population for peptide HPTGluArg (Table 1, 42 ± 2 %) was slightly higher compared to that for peptide HPTGluLys (38 ± 1 %) (Kuo et al. 2013a), most likely due to the slightly higher strand propensity for Arg compared to Lys at position 9 (fraction folded population of HPTAlaLys and HPTAlaArg were 22 ± 2 and 27 ± 2 %, respectively) (Kuo et al. 2013b). Furthermore, these fraction folded populations are consistent with a report on similar peptides (VK and VR) (Tatko and Waters 2003). The fraction folded population for all HPTZbbAgx peptides was between 28 and 56 % (Table 1). This range for the fraction folded population can be rationalized by considering the sheet/strand propensity of the individual Arg and Glu analogs, the diagonal Thr2-Agx9 interaction, and the lateral Zbb4-Agx9 interactions. The overall range of the fraction folded population for the HPTZbbAgx peptides with Arg analogs was more narrow compared to that for the HPTZbbXaa peptides with Lys analogs (between 24 and 63 %), suggesting the difference between the guanidinium and ammonium functionalities (Kuo et al. 2013a).

The thermodynamic strand propensity of the negatively charged residues at position 4 decreased with increasing side chain length (Kuo et al. 2013b). In addition, the strand propensity for Agx residues at position 9 followed the trend Agh > Arg ~ Agp > Agb (Kuo et al. 2013b). As such, it is not surprising that peptide HPTAadAgb exhibited the lowest fraction folded population (28 ± 3 %; Table 1; Fig. 3), because Aad and Agb exhibited the lowest strand propensity among the analogous charged residues at positions 4 and 9, respectively. Similarly, since both of Asp and Agh residues exhibited the highest strand propensity among the analogous charged residues at positions 4 and 9, respectively, peptide HPTAspAgh exhibited the highest fraction folded population (56 ± 1 %; Table 1; Fig. 3). Apparently, the strand propensity of the charged residues is the dominant factor for the fraction folded population of these hairpin peptides.

The fraction folded populations of peptides HPTAspAgp, HPTGluAgp, and HPTAadAgp were 52, 47, and 37 %, respectively (Table 1; Fig. 3), consistent with the trend for the strand propensity of the negatively charged residues at position 4 (Kuo et al. 2013b). However, among the three HPTZbbArg peptides, peptide HPTGluArg exhibited the least fraction folded population (Table 1; Fig. 3). Similarly, peptide HPTGluAgh exhibited the least fraction folded population among the three HPTZbbAgh peptides

(Table 1; Fig. 3). As such, the fraction folded trend for the HPTZbbArg and HPTZbbAgh peptides did not follow the strand propensity trend of the negatively charged residues at position 4. Since the three HPTZbbArg peptides exhibited NOE cross peaks between Thr2 and Arg9 in the ROESY spectra (Figs. S5B, S9B, S13B), the Thr2-Arg9 diagonal interactions should be similar. Therefore, the difference in the fraction folded population for the HPTZbbArg peptides should be due to the sheet/strand propensity of the negatively charged residue at position 4, and the lateral interactions between the side chains of Zbb4 and Arg9. This is also the case for the HPTZbbAgh peptides. Accordingly, the lateral Zbb4-Arg9 and Zbb4-Agh9 interactions should contribute to the β-hairpin stability.

The Asp-containing HPTZbbAgx peptides exhibited higher fraction folded populations compared to the corresponding Glu- and Aad-containing peptides. This was consistent with the higher strand propensity for Asp at position 4 compared to both Glu and Aad (Kuo et al. 2013b). Furthermore, for both the HPTGluAgx and HPTAadAgx peptides, the Agp-containing peptides exhibited exceptionally high fraction folded populations, most likely caused by the higher than expected strand propensity for Agp at position 9 (Kuo et al. 2013b). The short Asp and Agp side chains bring the branched bulky carboxylate and guanidinium groups close to the backbone, respectively, to limit the backbone conformations to sheet-like structures through steric interactions with the backbone (Bai and Englander 1994; Street and Mayo 1999; Kuo et al. 2013b). Furthermore, these short side chains could potentially hydrogen bond to the backbone to stabilize the strand conformation with less entropic penalty compared to the longer side chains. Accordingly, lengthening Agp by only one methylene to Agb in the HPTGluAgx and HPTAadAgx peptides significantly lowered the fraction folded populations (Table 1; Fig. 3). The low fraction folded population for these Agb-containing peptides is consistent with the low strand propensity for the positively charged residue Agb at position 9. However, the number of Thr2-Agx9 diagonal NOE connectivities suggested a stronger diagonal Thr2-Agx9 interaction for Agp compared to Agb (Fig. 4a, b). In contrast, for the HPTAspAgx peptides, the positively charged residue Agp could be lengthened by one methylene to Agb while maintaining a high fraction folded population (Table 1; Fig. 3). This clearly did not follow the strand propensity trend for the positively charged residues at position 9. Based on the number of diagonal Thr2-Agx9 NOE connectivities, the cross-strand Thr2-Agx9 interactions may have increased with increasing side chain length to stabilize the hairpin structure (Fig. 4c, d). Nonetheless, a more stabilizing lateral Asp4-Agb9 interaction compared to the Asp4-Agp9 interaction could not be completely ruled out.

In α-helices, intra-helical ion pairing interactions can contribute up to −0.8 kcal/mol to helix stability (Smith and Scholtz 1998; Cheng et al. 2007). In β-hairpin peptides, ion pairing interactions have shown to provide −0.1 to −0.4 kcal/mol stability (de Alba et al. 1995; Searle et al. 1999; Ramirez-Alvarado et al. 2001; Ciani et al. 2003; Kiehna and Waters 2003). The effect of charged amino acid side chain length on lateral cross-strand interactions between carboxylate-containing residues (Glu analogs) and ammonium-containing residues (Lys analogs) has been previously investigated (Kuo et al. 2013a). The values were mostly consistent with earlier reports except for the extraordinary stabilizing lateral Glu-Dap interaction, which provided up to −0.83 kcal/mol to the hairpin stability (Kuo et al. 2013a). Various side chain lengths of the oppositely charged amino acids for intra-helical carboxylate-guanidinium (Zbb-Agx) ion pairing interaction energy has provided up to −0.3 kcal/mol (Asp-Agp ion pair) to helix stability (Kuo et al. 2014). The ion pairing interaction energy (ΔG_{int}) in this study for cross-strand lateral Zbb-Agx in a β-hairpin was also consistent with reported literature values for analogous Glu-Lys interactions (Ramirez-Alvarado et al. 2001; Kiehna and Waters 2003; Ciani et al. 2003; Kuo et al. 2013a). Although the values for the Zbb-Agx ion pairing interactions were mostly non-existent (Table 2), this apparent lack of interaction energy between two oppositely charged residues only indicates minimal variation in coupling energy but does not mean the residues are not coupled to one another.

Cross-strand lateral interactions seemed to exist for Asp-Agb, Glu-Agp, Aad-Arg, and Aad-Agh pairs in the HPTZbbAgx peptides based on the interaction energy from double mutant cycle analyses (ΔG_{int}, Table 2). However, upon considering the standard deviations, only the Aad-Arg and Aad-Agh interactions were clearly stabilizing. For cross-strand lateral interactions between Glu analogs and Lys analogs (Kuo et al. 2013a), smaller number of side chain methylenes appeared to provide more side chain rigidity (Kuo et al. 2013a), leading to stronger lateral ion pairing interactions due to less entropic penalty upon forming an ion pair. Furthermore, electrostatics appeared to dominate the lateral cross-strand ion pairing interaction between residues with short side chains (Kuo et al. 2013a). However, none of the lateral Zbb-Agx ion pairs with shorter side chains for both charged residues exhibited stabilizing energetics for the β-hairpin structure. Although the lateral Glu-Dap ion pairing interaction provided −0.83 kcal/mol to hairpin stability (Kuo et al. 2013a), the lateral Glu-Agp ion pair interaction was essentially non-existent in this study, despite involving the exact same number of methylenes for the potentially interacting residues. This difference must be due to the difference between the guanidinium-bearing side chain of Agp residue and ammonium-bearing side chain of

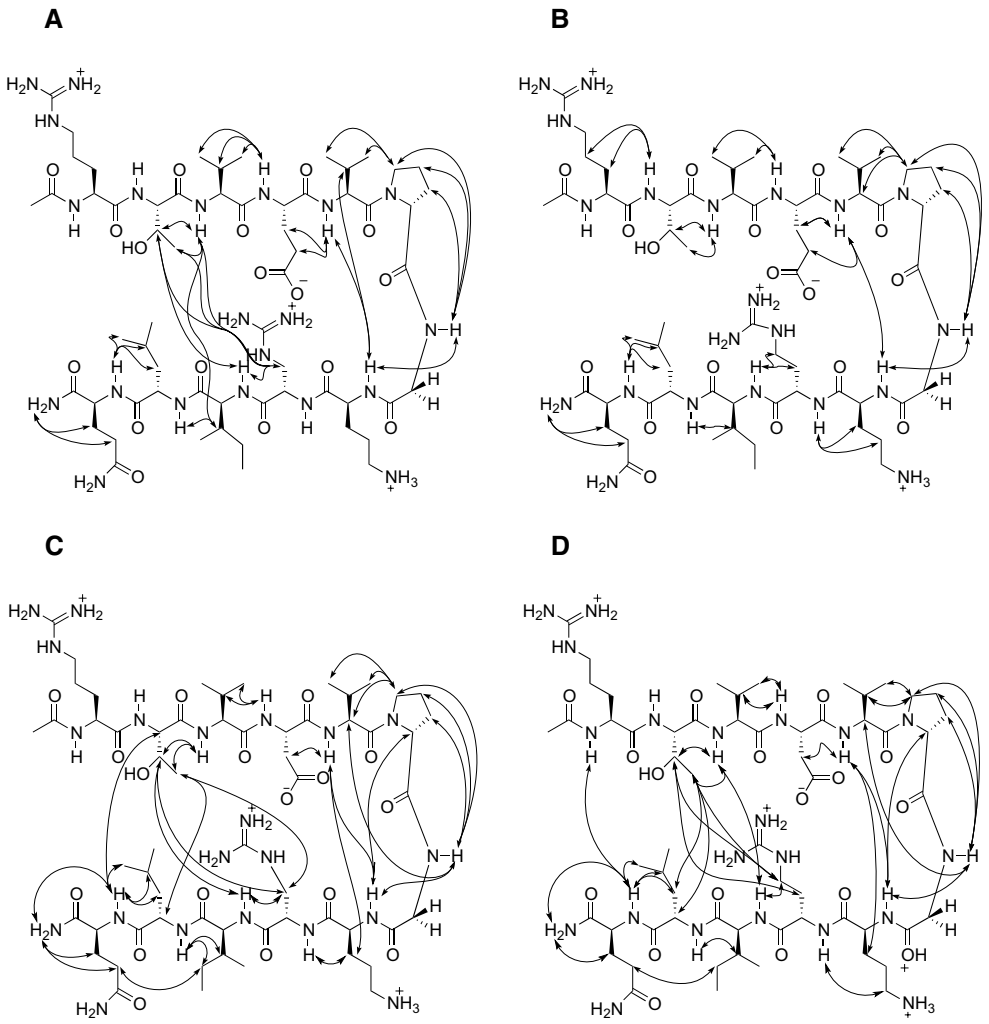

Fig. 4 The inter-residue NOEs involving side chain protons for peptides HPTGluAgp (**a**), HPTGluAgb (**b**), HPTAspAgp (**c**), and HPTAspAgb (**d**)

Dap. The more diffuse positive charge for the guanidinium group compared to the ammonium group may result in a weaker electrostatic Glu-Agp interaction compared to Glu-Dap interaction. Based on this reason, the short guanidinium-containing amino acids might not be suitable to form cross-strand lateral ion pairing interactions based on electrostatics. Furthermore, the lack of cross-strand lateral ion pairing interactions between the natural residues Asp/Glu and Arg could be attributed to weakened electrostatics due to the diffuse positive charge on the guanidinium group, insufficient number of methylenes for potential hydrophobic interactions, or the entropic penalty for ion pairing involving the lengthy Arg side chain.

The ΔG_{int} values suggested that combinations with longer side chains for both charged residues such as Aad-Arg/Agh ion pairs stabilized the β-hairpin, consistent with our study on the lateral Glu-Lys ion pairing interactions with various side chain lengths (Kuo et al. 2013a), showing that combinations of longer side chains such as Aad-Orn/Lys stabilized the β-hairpin structure (Kuo et al. 2013a). The longer negatively charged residue Aad side chain with more methylenes could potentially participate in hydrophobic interactions with the longer positively charged residues Arg and Agh. In addition, the longer side chain of Aad may serve as a spacer to separate the electron withdrawing backbone from the carboxylate, and the more methylenes provide an electron-donating group for the carboxylate group to enable stronger electrostatic interactions with the positively charged residues. However, the longer side chain of both charged residues would provide more flexibility to increase the entropic penalty upon forming an ion pair. Nonetheless, the main contribution to the stabilizing lateral Aad-Arg/Agh cross-strand ion pairing interactions was perhaps hydrophobics, based on the apparent hydrophobic nature for the analogous stabilizing energetics for the Aad-Orn/Lys interactions (Kuo et al. 2013a). Although the

Table 3 Survey results on lateral antiparallel cross-strand sequence patterns

Position *i*	Position *j*	Context[b]	Strand context[a]	No.[a]	Sheet pair propensity[c]	*Z* value	*P* value	Salt bridge[d]
Asp	Arg	NHB–NHB	Internal–internal	46	0.99 ± 0.14	−0.10	9.21×10^{-1}	30
Glu	Arg	NHB–NHB	Internal–internal	75	1.36 ± 0.18	2.69	7.19×10^{-3}	31
Asp	Arg	HB–HB	Internal–internal	29	0.61 ± 0.09	−2.70	7.01×10^{-3}	5
Glu	Arg	HB–HB	Internal–internal	117	2.08 ± 0.28	8.19	2.71×10^{-16}	45
Asp	Arg	NHB–NHB	Edge–edge	46	0.94 ± 0.13	−0.41	6.79×10^{-1}	16
Glu	Arg	NHB–NHB	Edge–edge	77	1.34 ± 0.18	2.55	1.09×10^{-2}	15
Asp	Arg	HB–HB	Edge–edge	54	1.09 ± 0.15	0.66	5.12×10^{-1}	8
Glu	Arg	HB–HB	Edge–edge	115	1.97 ± 0.26	7.43	1.05×10^{-13}	36
Asp	Arg	NHB–NHB	Internal–edge	38	0.63 ± 0.08	−2.83	4.70×10^{-3}	21
Glu	Arg	NHB–NHB	Internal–edge	94	1.33 ± 0.16	2.78	5.46×10^{-3}	23
Asp	Arg	HB–HB	Internal–edge	33	0.56 ± 0.07	−3.35	8.18×10^{-4}	16
Glu	Arg	HB–HB	Internal–edge	142	2.05 ± 0.25	8.69	3.54×10^{-18}	59
Asp	Arg	NHB–NHB	Edge–internal	74	1.23 ± 0.16	1.83	6.79×10^{-15}	43
Glu	Arg	NHB–NHB	Edge–internal	140	1.98 ± 0.24	8.26	1.45×10^{-40}	58
Asp	Arg	HB–HB	Edge–internal	60	1.02 ± 0.13	0.18	8.59×10^{-1}	17
Glu	Arg	HB–HB	Edge–internal	182	2.63 ± 0.32	13.4	3.20×10^{-41}	63

[a] The occurrence of oppositely charged residues on antiparallel neighboring strands in the non-redundant protein structure database PDBselect (April 2009, 25 % threshold) (Hobohm and Sander 1994; Griep and Hobohm 2010). The β-strand conformation was defined based on DSSP (Kabsch and Sander 1983; Joosten et al. 2011). The residues on an internal strand and an edge strand were defined based on the presence of complementary strands on both sides and on only one side using DSSP, respectively (Kabsch and Sander 1983; Joosten et al. 2011). The antiparallel and parallel orientations were defined based on DSSP (Kabsch and Sander 1983; Joosten et al. 2011)

[b] The non-hydrogen-bonded (NHB) and hydrogen-bonded (HB) residues were defined based on the hydrogen bond definition using DSSP (Kabsch and Sander 1983; Joosten et al. 2011)

[c] The occurrence for the various sequence patterns divided by the corresponding expected value. The expected value was obtained by bootstrapping the complete PDBselect database, thereby including the bias for the occurrence of each residue for the sheet conformation. Since bootstrapping was performed 100,000 times, this enabled the calculation of a standard deviation for the expected value and thus the sheet pair propensity

[d] The number of the occurrences for each sequence pattern that actually forms salt bridges between the oppositely charged side chain functionalities. The presence of a salt bridge is defined by an N–O distance less than or equal to 3 Å

overall length of Aad-Agp/Agb ion pairs was the same as the Aad-Orn/Lys ion pairs, the Aad-Agp/Agb ion pairs did not exhibit stabilizing interaction energetics. In contrast, Aad-Arg/Agh ion pairs exhibited the similar ion pairing interaction energy compared to Aad-Orn/Lys even though the overall lengths are different. This might be because the Arg/Agh and Orn/Lys have the same number of methylenes to interact with the negatively charged residue Aad, resulting in similar hydrophobic interaction energetics to stabilize the β-hairpin structure. Based on this, long side chains with the same number of methylenes differing in functional groups provide similar ion pairing interaction energy. Also, the main contribution to the lateral Zbb-Agx cross-strand ion pairing interaction was apparently hydrophobics for the longer side chains (Aad-Arg/Agh). Importantly, the side chain length matching for the long oppositely charged residues on lateral cross strands appeared to be critical for providing stabilizing energetics in β-hairpin structures.

A survey was performed on the non-redundant protein structure database PDBselect (April 2009, 25 % threshold) (Hobohm and Sander 1994; Griep and Hobohm 2010), to provide further insight into the utilization of lateral Asp-Arg and Glu-Arg ion pairs on antiparallel strands in sheet structures of natural proteins. A total of 4,418 protein chains involving 666,086 residues were considered. There were 150,934 residues that adopted a sheet conformation. The sheet pair propensity for each sequence pattern was derived from the expected occurrence in all structures to represent how frequently a particular sequence pattern occurred in a sheet conformation compared to all structures in the database. The statistical sheet propensity for the charged residues followed the trends Glu > Asp and Lys > Arg (Kuo et al. 2013b). The lateral sheet pair propensity in antiparallel strands was consistent with the sheet propensity, exhibiting the trend Glu-Arg > Asp-Arg regardless of context (edge or internal strands, non-hydrogen-bonded or hydrogen-bonded positions) (Table 3), suggesting the importance of length matching. The same trend was observed when the potential ion pairs involving antiparallel orientation with only edge strands at non-hydrogen-bonded positions, which is the same as our experimental sequence pattern in the β-hairpin model. Besides, the statistical

sheet pair propensity at non-hydrogen-bonded positions on edge strands in antiparallel sheets followed the trend Asp-Lys > Asp-Arg, and Glu-Lys > Glu-Arg (Kuo et al. 2013a). The number of salt bridges varied depending on context. Although the Asp-Arg sheet pair propensity on the edge strands at non-hydrogen-bonded positions was less than the Glu-Arg pair, the number of salt bridges for the Asp-Arg pair was similar to the Glu-Arg pair. Interestingly, the occurrence of the Asp-Arg and Glu-Arg pairs on the edge strand at non-hydrogen-bonded positions was less than Asp-Lys and Glu-Lys, respectively. Furthermore, the number of salt bridges for the Asp-Lys was higher than the Asp-Arg pair. In contrast, the number of salt bridges for the Glu-Lys was less than the Glu-Arg pair. Importantly, the statistical sheet pair propensity trends appeared to suggest the importance of length matching.

Conclusion

The effect of varying the side chain length on ion pairing interactions between carboxylate- and guanidinium-bearing residues at lateral non-hydrogen-bonded positions on the two antiparallel strands in a β-hairpin has been studied. Peptide HPTAspAgh exhibited the highest fraction folded population due to the highest sheet propensity of Asp and Agh residues at the corresponding positions compared to the analogous charged residues with different side chain lengths, respectively. Both the shortest Agp and Asp residues bring the branched bulky group close to the backbone to limit the backbone conformations to sheet-like structures perhaps through steric interactions with the backbone, or through stabilizing side chain–main chain hydrogen bonds with minimal entropic penalty. Accordingly, the fraction folded populations of the peptides containing the shorter Asp were distinctly higher than that of the peptides containing the two longer negatively charged residues Glu and Aad. Similarly, the Agp-containing peptides exhibited exceptionally high fraction folded populations compared to peptides containing other Arg analogs. However, ion pairing combinations involving shorter side chains for both charged residues such as Asp/Glu-Agp did not exhibit stabilizing energetics, most likely due to the weakened electrostatic interactions between the diffuse positive charge on the guanidinium group and the negative charge on the carboxylate. Hence, the guanidinium-bearing residues might not be suitable for relying on electrostatics to interact with carboxylate-bearing residues to stabilize a β-hairpin. Instead, ion pair combinations involving longer side chains for both charged residues such as Aad-Arg/Agh stabilized the β-hairpin structure, perhaps due to hydrophobics. The survey on natural proteins revealed that the sheet pair propensity followed the trends Asp-Arg < Glu-Arg. As such, side chain length matching for the long oppositely charged residues on separate strands appears to be important for providing stabilizing energetics in β-hairpin structures. Importantly, these results should be useful in designing stable sheet structures by using charged residues with different functional group and varying side chain lengths to facilitate the modulation of β-sheet structure stability.

Acknowledgments This work was supported by National Taiwan University (R.P.C., NTU-ERP-103R891302) and the Ministry of Science and Technology in Taiwan (former National Science Council; S. J. H., 100-2731-M-002-002-MY2; R.P.C., 99-2113-M-002-002-MY2, 101-2113-M-002-006-MY2, 103-2113-M-002-018-MY3). The authors would like to thank the Computer and Information Networking Center at National Taiwan University for the support of the high-performance computing facilities.

Conflict of interest The authors declare that they have no conflict of interest.

References

Arakawa T, Tsumoto K (2003) The effects of arginine on refolding of aggregated proteins: Not facilitate refolding, but suppress aggregation. Biochem Biophys Res Commun 304:148–152

Argos P (1988) An investigation of protein subunit and domain interfaces. Protein Eng 2:101–113

Arora D, Khanna N (1996) Method for increasing the yield of properly folded recombinant human gamma interferon from inclusion bodies. J Biotechnol 52:127–133

Atherton E, Fox H, Harkiss D, Logan CJ, Sheppard RC, Williams BJ (1978) A mild procedure for solid-phase peptide-synthesis—Use of the fluorenylmethoxycarbonyl amino acids. J Chem Soc Chem Commun 13:537–539. doi:10.1039/C39780000537

Aue WP, Bartholdi E, Ernst RR (1976) 2-Dimensional spectroscopy—application to nuclear magnetic-resonance. J Chem Phys 64(5):2229–2246. doi:10.1063/1.432450

Augustyns K, Kraas W, Jung G (1998) Investigation on the stability of the Dde protecting group used in peptide synthesis: migration to an unprotected lysine. J Pept Res 51:127–133

Bai Y, Englander SW (1994) Hydrogen bond strength and β-sheet propensities: the role of a side chain blocking effect. Proteins 18(3):262–266. doi:10.1002/prot.340180307

Baldwin RL, Rose GD (1999a) Is protein folding hierarchic? I. Local structure and peptide folding. Trends Biochem Sci 24(1):26–33. doi:10.1016/S0968-0004(98)01346-2

Baldwin RL, Rose GD (1999b) Is protein folding hierarchic? II. Folding intermediates and transition states. Trends Biochem Sci 24(2):77–83. doi:10.1016/S0968-0004(98)01345-0

Bartzokis G, Lu PH, Mintz J (2007) Human brain myelination and amyloid β deposition in Alzheimer's disease. Alzheimers Dement 3(2):122–125. doi:10.1016/j.jalz.2007.01.019

Bax A, Davis DG (1985) MLEV-17-based two-dimensional homonuclear magnetization transfer spectroscopy. J Magn Reson 65(2):355–360. doi:10.1016/0022-2364(85)90018-6

Blasie CA, Berg JM (1997) Electrostatic interactions across a β-sheet. Biochemistry 36(20):6218–6222. doi:10.1021/bi962805i

Bogan AA, Thorn KS (1998) Anatomy of hot spots in protein interfaces. J Mol Biol 280:1–9

Bothner-By AA, Stephens RL, Lee J-M, Warren CD, Jeanloz RW (1984) Structure determination of a tetrasaccharide—transient

nuclear overhauser effects in the rotating frame. J Am Chem Soc 106(3):811–813. doi:10.1021/Ja00315a069
Chakrabartty A, Kortemme T, Baldwin RL (1994) Helix propensities of the amino acids measured in alanine-based peptides without helix-stabilizing side-chain interactions. Protein Sci 3(5):843–852. doi:10.1002/pro.5560030514
Cheng RP, Girinath P, Ahmad R (2007) Effect of lysine side chain length on intra-helical glutamate-lysine ion pairing interactions. Biochemistry 46(37):10528–10537. doi:10.1021/bi700701z
Cheng RP, Wang W-R, Girinath P, Yang P-A, Ahmad R, Li J-H, Hart P, Kokona B, Fairman R, Kilpatrick C, Argiros A (2012a) Effect of glutamate side chain length on intrahelical glutamate-lysine ion pairing interactions. Biochemistry 51(36):7157–7172. doi:10.1021/bi300655z
Cheng RP, Weng Y-J, Wang W-R, Koyack MJ, Suzuki Y, Wu C-H, Yang P-A, Hsu H-C, Kuo H-T, Girinath P, Fang C-J (2012b) Helix formation and capping energetics of arginine analogs with varying side chain length. Amino Acids 43(1):195–206. doi:10.1007/s00726-011-1064-2
Chou PY, Fasman GD (1974) Conformational parameters for amino acids in helical, β-sheet, and random coil regions calculated from proteins. Biochemistry 13(2):211–222
Ciani B, Jourdan M, Searle MS (2003) Stabilization of β-hairpin peptides by salt bridges: role of preorganization in the energetic contribution of weak interactions. J Am Chem Soc 125(30):9038–9047. doi:10.1021/ja030074l
Cockroft SL, Hunter CA (2007) Chemical double-mutant cycles: dissecting non-covalent interactions. Chem Soc Rev 36(2):172–188. doi:10.1039/B603842p
Cootes AP, Curmi PMG, Cunningham R, Donnelly C, Torda AE (1998) The dependence of amino acid pair correlations on structural environment. Proteins 32:175–189
Dalgarno DC, Levine BA, Williams RJ (1983) Structural information from NMR secondary chemical shifts of peptide α C-H protons in proteins. Biosci Rep 3(5):443–452
de Alba E, Blanco FJ, Jimenez MA, Rico M, Nieto JL (1995) Interactions responsible for the pH dependence of the β-hairpin conformational population formed by a designed linear peptide. Eur J Biochem 233(1):283–292
de Bernardez Clark E (1998) Refolding of recombinant proteins. Curr Opin Biotechnol 9:157–163
Doig AJ, Baldwin RL (1995) N- and C-capping preferences for all 20 amino acids in α-helical peptides. Protein Sci 4(7):1325–1336. doi:10.1002/pro.5560040708
Feichtinger K, Sings HL, Baker TJ, Matthews K, Goodman M (1998a) Triurethane-protected guanidines and triflyldiurethane-protected guanidines: new reagents for guanidinylation reactions. J Org Chem 63(23):8432–8439. doi:10.1021/Jo9814344
Feichtinger K, Zapf C, Sings HL, Goodman M (1998b) Diprotected triflylguanidines: a new class of guanidinylation reagents. J Org Chem 63(12):3804–3805. doi:10.1021/Jo980425s
Fields GB, Noble RL (1990) Solid phase peptide synthesis utilizing 9-fluorenylmethoxycarbonyl amino acids. Int J Pept Protein Res 35(3):161–214
Griep S, Hobohm U (2010) PDBselect 1992–2009 and PDBfilter-select. Nucleic Acids Res 38:D318–D319. doi:10.1093/nar/gkp786 (Database issue)
Haataja L, Gurlo T, Huang CJ, Butler PC (2008) Islet amyloid in type 2 diabetes, and the toxic oligomer hypothesis. Endocr Rev 29(3):303–316. doi:10.1210/er.2007-0037
Hardy J, Allsop D (1991) Amyloid deposition as the central event in the aetiology of Alzheimer's disease. Trends Pharmacol Sci 12(10):383–388
Hobohm U, Sander C (1994) Enlarged representative set of protein structures. Protein Sci 3(3):522–524. doi:10.1002/pro.5560030317
Höppener JW, Ahrén B, Lips CJ (2000) Islet amyloid and type 2 diabetes mellitus. N Engl J Med 343(6):411–419. doi:10.1056/NEJM200008103430607
Horovitz A (1996) Double-mutant cycles: a powerful tool for analyzing protein structure and function. Fold Des 1(6):R121–R126. doi:10.1016/S1359-0278(96)00056-9
Hu Z, Buyong M, Wolfson H, Nussinov R (2000) Conservation of polar residues as hot spots at protein interfaces. Proteins Struct Funct Genet 39:331–342
Hughes RM, Benshoff ML, Waters ML (2007) Effects of chain length and N-methylation on a cation–π interaction in a β-hairpin peptide. Chemistry 13(20):5753–5764. doi:10.1002/chem.200601753
Hutchinson EG, Sessions RB, Thornton JM, Woolfson DN (1998) Determinants of strand register in antiparallel β-sheets of proteins. Protein Sci 7(11):2287–2300. doi:10.1002/pro.5560071106
Irvine GB, El-Agnaf OM, Shankar GM, Walsh DM (2008) Protein aggregation in the brain: the molecular basis for Alzheimer's and Parkinson's diseases. Mol Med 14(7–8):451–464. doi:10.2119/2007-00100.Irvine
Ito L, Kobayashi T, Shiraki K, Yamaguchi H (2008) Effect of amino acids and amino acid derivatives on crystallization of hemoglobin and ribonuclease A. J Synchrotron Radiat 15:316–318
Janin J, Miller S, Chothia C (1988) Surface, subunit interfaces and interior of oligomeric proteins. J Mol Biol 204:155–164
Jeener J, Meier BH, Bachmann P, Ernst RR (1979) Investigation of exchange processes by 2-dimensional NMR-spectroscopy. J Chem Phys 71(11):4546–4553. doi:10.1063/1.438208
Jones S, Thornton JM (1995) Protein–protein interactions: a review of protein dimer structures. Prog Biophys Mol Biol 63:31–65
Joosten RP, Beek TAHT, Krieger E, Hekkelman ML, Hooft RWW, Schneider R, Sander C, Vriend G (2011) A series of PDB related databases for everyday needs. Nucleic Acids Res 39:D411–D419. doi:10.1093/Nar/Gkq1105
Kabsch W, Sander C (1983) Dictionary of protein secondary structure—pattern-recognition of hydrogen-bonded and geometrical features. Biopolymers 22(12):2577–2637. doi:10.1002/Bip.360221211
Kiehna SE, Waters ML (2003) Sequence dependence of β-hairpin structure: comparison of a salt bridge and an aromatic interaction. Protein Sci 12(12):2657–2667. doi:10.1110/ps.03215403
Kim CA, Berg JM (1993) Thermodynamic β-sheet propensities measured using a zinc-finger host peptide. Nature 362(6417):267–270. doi:10.1038/362267a0
Kim YM, Prestegard JH (1989) Measurement of vicinal couplings from cross peaks in COSY spectra. J Magn Reson 84(1):9–13. doi:10.1016/0022-2364(89)90003-6
Kim E, Paliwal S, Wilcox CS (1998) Measurements of molecular electrostatic field effects in edge-to-face aromatic interactions and CH–π interactions with implications for protein folding and molecular recognition. J Am Chem Soc 120(43):11192–11193
Kitamoto T, Tateishi J, Tashima T, Takeshita I, Barry RA, DeArmond SJ, Prusiner SB (1986) Amyloid plaques in Creutzfeldt-Jakob disease stain with prion protein antibodies. Ann Neurol 20(2):204–208. doi:10.1002/ana.410200205
Kuo H-T, Fang C-J, Tsai H-Y, Yang M-F, Chang H-C, Liu S-L, Kuo L-H, Wang W-R, Yang P-A, Huang S-J, Huang S-L, Cheng RP (2013a) Effect of charged amino acid side chain length on lateral cross-strand interactions between carboxylate-containing residues and lysine analogues in a β-hairpin. Biochemistry 52(51):9212–9222. doi:10.1021/bi400974x
Kuo L-H, Li J-H, Kuo H-T, Hung C-Y, Tsai H-Y, Chiu W-C, Wu C-H, Wang W-R, Yang P-A, Yao Y-C, Wong T-W, Huang S-J, Huang S-L, Cheng RP (2013b) Effect of charged amino acid side chain length at non-hydrogen bonded strand positions on β-hairpin stability. Biochemistry 52:7785–7797

Kuo H-T, Yang P-A, Wang W-R, Hsu H-C, Wu C-H, Ting Y-T, Weng M-H, Kuo L-H, Cheng RP (2014) Effect of side chain length on intrahelical interactions between carboxylate- and guanidinium-containing amino acids. Amino Acids 46(8):1867–1883. doi:10.1007/s00726-014-1737-8

Laughrey ZR, Kiehna SE, Riemen AJ, Waters ML (2008) Carbohydrate-π Interactions: what are they worth? J Am Chem Soc 130(44):14625–14633

Mastaglia FL, Johnsen RD, Byrnes ML, Kakulas BA (2003) Prevalence of amyloid-β deposition in the cerebral cortex in Parkinson's disease. Mov Disord 18(1):81–86. doi:10.1002/mds.10295

Merkel JS, Sturtevant JM, Regan L (1999) Sidechain interactions in parallel β sheets: the energetics of cross-strand pairings. Structure 7(11):1333–1343

Minor DL, Kim PS (1994) Measurement of the β-sheet-forming propensities of amino acids. Nature 367(6464):660–663. doi:10.1038/367660a0

Mitchell DJ, Kim DT, Steinman L, Fathman CG, Rothbard JB (2000) Polyarginine enters cells more efficiently than other polycationic homopolymers. J Pept Res 56:318–325

Munoz V, Serrano L (1994) Intrinsic secondary structure propensities of the amino acids, using statistical φ–ψ matrices: comparison with experimental scales. Proteins 20(4):301–311. doi:10.1002/prot.340200403

Namba Y, Tomonaga M, Kawasaki H, Otomo E, Ikeda K (1991) Apolipoprotein E immunoreactivity in cerebral amyloid deposits and neurofibrillary tangles in Alzheimer's disease and kuru plaque amyloid in Creutzfeldt-Jakob disease. Brain Res 541(1):163–166

Padmanabhan S, York EJ, Stewart JM, Baldwin RL (1996) Helix propensities of basic amino acids increase with the length of the side-chain. J Mol Biol 257(3):726–734. doi:10.1006/jmbi.1996.0197

Paliwal S, Geib S, Wilcox CS (1994) Chemistry of synthetic receptors and functional-group arrays.24. Molecular torsion balance for weak molecular recognition forces—effects of tilted-T edge-to-face aromatic interactions on conformational selection and solid-state structure. J Am Chem Soc 116(10):4497–4498

Ramirez-Alvarado M, Blanco FJ, Serrano L (1996) De novo design and structural analysis of a model β-hairpin peptide system. Nat Struct Biol 3(7):604–612

Ramirez-Alvarado M, Kortemme T, Blanco FJ, Serrano L (1999) β-Hairpin and β-sheet formation in designed linear peptides. Bioorg Med Chem 7(1):93–103

Ramirez-Alvarado M, Blanco FJ, Serrano L (2001) Elongation of the BH8 β-hairpin peptide: electrostatic interactions in β-hairpin formation and stability. Protein Sci 10(7):1381–1392. doi:10.1110/Ps.52901

Rose GD, Gierasch LM, Smith JA (1985) Turns in peptides and proteins. Adv Protein Chem 37:1–109

Russell SJ, Cochran AG (2000) Designing stable β-hairpins: energetic contributions from cross-strand residues. J Am Chem Soc 122(50):12600–12601

Russell SJ, Blandl T, Skelton NJ, Cochran AG (2003) Stability of cyclic β-hairpins: asymmetric contributions from side chains of a hydrogen-bonded cross-strand residue pair. J Am Chem Soc 125(2):388–395. doi:10.1021/Ja028075i

Scherzinger E, Lurz R, Turmaine M, Mangiarini L, Hollenbach B, Hasenbank R, Bates GP, Davies SW, Lehrach H, Wanker EE (1997) Huntingtin-encoded polyglutamine expansions form amyloid-like protein aggregates in vitro and in vivo. Cell 90(3):549–558

Searle MS, Griffiths-Jones SR, Skinner-Smith H (1999) Energetics of weak interactions in a β-hairpin peptide: electrostatic and hydrophobic contributions to stability from lysine salt bridges. J Am Chem Soc 121(50):11615–11620

Singh SM, Panda AK (2005) Solubilization and refolding of bacterial inclusion body proteins. J Biosci Bioeng 99:303–310

Smith CK, Regan L (1995) Guidelines for protein design: the energetics of β sheet side chain interactions. Science 270(5238):980–982

Smith JS, Scholtz JM (1998) Energetics of polar side-chain interactions in helical peptides: salt effects on ion pairs and hydrogen bonds. Biochemistry 37(1):33–40. doi:10.1021/bi972026h

Smith CK, Withka JM, Regan L (1994) A thermodynamic scale for the β-sheet forming tendencies of the amino acids. Biochemistry 33(18):5510–5517

Stanger HE, Gellman SH (1998) Rules for antiparallel β-sheet design: d-Pro-Gly is superior to L-Asn-Gly for β-hairpin nucleation. J Am Chem Soc 120(17):4236–4237

Street AG, Mayo SL (1999) Intrinsic β-sheet propensities result from van der Waals interactions between side chains and the local backbone. Proc Natl Acad Sci USA 96(16):9074–9076

Sueki M, Lee S, Powers SP, Denton JB, Konishi Y, Scheraga HA (1984) Helix coil stability constants for the naturally-occurring amino-acids in water. 22. Histidine parameters from random poly[(hydroxybutyl)glutamine-co-L-histidine]. Macromolecules 17(2):148–155. doi:10.1021/Ma00132a006

Syud FA, Espinosa JF, Gellman SH (1999) NMR-based quantification of β-sheet populations in aqueous solution through use of reference peptides for the folded and unfolded states. J Am Chem Soc 121(49):11577–11578

Syud FA, Stanger HE, Gellman SH (2001) Interstrand side chain-side chain interactions in a designed β-hairpin: significance of both lateral and diagonal pairings. J Am Chem Soc 123(36):8667–8677

Tatko CD, Waters ML (2002) Selective aromatic interactions in β-hairpin peptides. J Am Chem Soc 124(32):9372–9373

Tatko CD, Waters ML (2003) The geometry and efficacy of cation–π interactions in a diagonal position of a designed β-hairpin. Protein Sci 12(11):2443–2452. doi:10.1110/ps.03284003

Tatko CD, Waters ML (2004) Comparison of C-H…π and hydrophobic interactions in a β-hairpin peptide: impact on stability and specificity. J Am Chem Soc 126(7):2028–2034. doi:10.1021/Ja038258n

Truant R, Atwal RS, Desmond C, Munsie L, Tran T (2008) Huntington's disease: revisiting the aggregation hypothesis in polyglutamine neurodegenerative diseases. FEBS J 275(17):4252–4262. doi:10.1111/j.1742-4658.2008.06561.x

Tsai C-J, Lin SL, Wolfson HJ, Nussinov R (1997) Studies of protein-protein interfaces: a statistical analysis of the hydrophobic effect. Protein Sci 6:53–64

Tsumoto K, Umetsu M, Kumagai I, Ejima D, Philo JS, Arakawa T (2004) Role of arginine in protein refolding, solubilization, and purification. Biotechnol Progr 20:1301–1308

Umetsu M, Tsumoto K, Hara M, Ashish K, Goda S, Adschiri T, Kumagai I (2003) How additives influence the refolding of immunoglobulin-folded proteins in a stepwise dialysis system. Spectroscopic evidence for highly efficient refolding of a single-chain Fv fragment. J Biol Chem 278:8979–8987

Volkmer-Engert R, Landgraf C, Schneider-Mergener J (1998) Charcoal surface-assisted catalysis of intramolecular disulfide bond formation in peptides. J Pept Res 51(5):365–369

Wender PA, Mitchell DJ, Pattabiraman K, Pelkey ET, Steinman L, Rothbard JB (2000) The design, synthesis, and evaluation of molecules that enable or enhance cellular uptake: peptoid molecular transporters. Proc Natl Acad Sci USA 97:13003–13008

Wender PA, Galliber WC, Goun EA, Jones LR, Pillow TH (2008) The design of guanidinium-rich transporters and their internalization mechanisms. Adv Drug Del Chem 60:452–472

Wishart DS, Sykes BD, Richards FM (1991) Relationship between nuclear magnetic resonance chemical shift and protein secondary structure. J Mol Biol 222(2):311–333. doi:10.1016/0022-2836(91)90214-Q

Wouters MA, Curmi PMG (1995) An analysis of side chain interactions and pair correlations within antiparallel β-sheets: the

differences between backbone hydrogen-bonded and non-hydrogen-bonded residue pairs. Proteins 22(2):119–131. doi:10.1002/Prot.340220205

Wu C-H, Chen Y-P, Mou C-Y, Cheng RP (2013) Altering the Tat-derived peptide bioactivity landscape by changing the arginine side chain length. Amino Acids 44(2):473–480. doi:10.1007/S00726-012-1357-0

Wüthrich K (1986) NMR of proteins and nucleic acids. Wiley, New York

Yao J, Dyson HJ, Wright PE (1997) Chemical shift dispersion and secondary structure prediction in unfolded and partly folded proteins. FEBS Lett 419(2–3):285–289. doi:10.1016/S0014-5793(97)01474-9